Synthetic lethality screening reveals FDA-approved drugs that overcome ATP7B-mediated tolerance of tumor cells to cisplatin

Marta Mariniello[1*], Raffaella Petruzzelli[1*], Luca G. Wanderlingh[1], Raffaele La Montagna[1], Annamaria Carissimo[1], Francesca Pane[2], Angela Amoresano[2], Diego Medina[1], Roman S. Polishchuk[1, #]

Affiliations:

[1] Telethon Institute of Genetics and Medicine, Pozzuoli, Naples, Italy

[2] Department of Chemistry, University Federico II, Naples, Italy

*co-first authors listed in alphabetical order

corresponding author: polish@tigem.it

ABSTRACT

Resistance of tumors to chemotherapy represents an important challenge in the modern oncology. Although platinum (Pt)-based drugs demonstrated excellent therapeutic potential their effectiveness in a wide range of tumors is limited by the development of resistance mechanisms. One of these mechanisms includes increased cisplatin sequestration/efflux by copper-transporting ATPase, ATP7B. In fact, ATP7B expression has been identified as a hallmark of chemotherapy-resistant tumors. However, targeting the ATP7B for reduction of Pt-tolerance in tumors represents a serious risk because suppression of ATP7B might compromise copper homeostasis like it happens in Wilson disease.

To circumvent ATP7B-mediated Pt tolerance we employed a high-throughput screening (HTS) of FDA/EMA-approved drug library to discover new therapeutic molecules that promote cisplatin toxicity in resistant ovarian carcinoma IGROV-CP20 cell line. Through a synthetic lethality approach, three hits (Tranilast, Telmisartan and Amphotericin B) were detected and validated for their ability to reduce cisplatin resistance. All 3 drugs induced DNA damage and inhibited ATP7B trafficking in a tumor-specific manner. RNAseq analysis revealed Tranilast and Amphotericin B to affect expression of genes operating in several pathways that confer tolerance to cisplatin. In the case of Tranilast, these included key molecular players operating in the distribution of copper and platinum to different intracellular compartments. In particular, Tranilast was found to suppress ATOX1 and, as a consequence, ATOX1-mediated trafficking of ATP7B in response to cisplatin.

Considering well-known safety profiles and tolerability of Tranilast, Telmisartan and Amphotericin B these drugs emerge as attractive candidates, which might be used for rapid development of new therapeutic strategies to overcome resistance of tumors to Pt-based chemotherapy.

Key words: Cancer; Cisplatin Resistance; Copper Transporters; ATP7B; High Throughput Screening.

INTRODUCTION

Platinum (Pt)-based drugs have had a major impact in cancer medicine since they display excellent efficiency in the treatment of a wide variety of solid tumors including testicular, head and neck, lung, ovarian, and colon cancers (*1*). The mechanism by which these drugs exert their anti-tumor effects is defined by their capacity to form intra-strand DNA adducts, which ultimately culminate in tumor cell apoptosis (*2*). However, the final outcome of Pt-based therapy is often hampered by the development of drug resistance, which remains a significant obstacle to successful treatment in the clinic (*1-5*). Pt resistance usually emerges as a result of an orchestrated action of several pathways, which include a cytosolic inactivation of Pt by sulfur-containing molecules like glutathione and metallothionein, activated DNA repair or reduced platinum accumulation and reduced Pt accumulation (*1, 6, 7*). Among these mechanisms, reduced Pt accumulation heavily relies on variations in expression and activity of membrane copper transporters, CTR1 and CTR2, regulating Pt uptake across the plasma membrane (*8-10*) and the copper transporting ATPases, ATP7A and ATP7B, driving Pt export from the cell (*11, 12*). In particular, elevated expression of ATP7B has been evidently correlated with the worse outcomes of cisplatin chemotherapies in patients with ovarian cancer and non-small cell lung cancer (*11, 13, 14*).

Normally, ATP7B is expressed in the liver hepatocytes and operates to maintain copper homeostasis in the body. In response to Cu overload, ATP7B moves from the Golgi to endo-lysosomal structures, where it sequesters excess Cu and promotes its further excretion to the bile (*15, 16*). Loss of function mutations do not allow ATP7B to discharge Cu to the bile leading to severe Cu toxicosis known as Wilson disease (*17, 18*).

Similar ATP7B-dependent mechanism was proposed to reduce Pt toxicity in tumor cells. It has been hypothesized that ATP7B promotes sequestration of Pt within intracellular post-Golgi vesicles and/or excretion of Pt at the cell surface (*3, 11, 19*). In agreement with this hypothesis, extensive relocation of ATP7B from the Golgi to vesicular compartment was observed in Pt-

resistant tumor cells (*20*). In addition, ATP7B has been proposed to chelate Pt via the metal-binding domains presented in this protein, hence, reducing Pt toxicity (*21-23*). In this context, circumventing ATP7B-mediated resistance emerges as an attractive strategy to increase efficiency of Pt-based cancer therapies.

We reasoned that screening for FDA/EMA-approved drugs might offer an effective shortcut for identification of the safe molecules, which reduce tolerance to cisplatin in tumor cells. Considering that safety profiles of such drugs are well characterized, their repurposing for another therapeutic use significantly reduces a risk of failure due to eventual adverse events in patients (*24*). Therefore, the main objective of our study was to search for FDA-approved molecules capable of overcoming cisplatin resistance in ovarian cancer cell lines overexpressing ATP7B. Using a synthetic lethality screening we revealed and validated 3 hits, which significantly reduced ATP7B-mediated tolerance to cisplatin in ovarian cancer cells. The drugs acted via blocking ATP7B export from the Golgi and down-regulating large cohorts of genes, which belong to cisplatin-resistance pathways including DNA repair, quality control and autophagy (*25-28*). Our findings underscore the effectiveness of unbiased screening approach for drug repurposing studies and pinpoint bio-safe drug candidates to combat ATP7B-mediated resistance of tumors to cisplatin.

METHODS

Antibodies and Other Reagents

The full list of antibodies, small interfering RNAs (siRNAs), primers is provided in the Supplementary Methods.

Cell culture

Cisplatin-sensitive human ovarian cancer IGROV and A2780 cells, and corresponding cisplatin resistant lines IGROV-CP20 and A2780 were obtained from Dr. A Sood (University of Texas MD Anderson Cancer Center) and Dr. S. Howell (Moores UCSD Cancer Center). The cells were grown in RPMI supplemented with 15% FBS, 2mM L-glutamine, and 1% penicillin and streptomycin.

HepG2 cells were grown in DMEM supplemented with 10% FCS, 2 mM L-glutamine, and 1% penicillin and streptomycin.

RNA interference

Small interfering RNAs (siRNA) targeting the ATP7B and ATP7A, were purchased from Sigma-Aldrich (St. Louis, USA). Scrambled siRNAs were used as a negative control. IGROV-CP20 cells were transfected with siRNA using Lipofectamine RNAiMAX reagent (Invitrogen). After 48 hours of interference, the cells were treated with 50µM cisplatin for 24 h and MTT cell viability assay was then performed. SiRNA-treated cells were then prepared for quantitative real time PCR to analyze the efficiency of silencing of ATP7B and ATP7A.

RNA preparation and quantitative real time PCR (qRT-PCR)

To evaluate the mRNAs expression levels of ATP7B, ATP7A and CTR1 genes, total RNAs were extracted with RNeasy Protect Mini kits (Quiagen) from IGROV-CP20 and IGROV cells. RNAs were reverse-transcribed using QuantiTect Reverse Transcription kits (Qiagen). qRT-PCR experiments were performed using Light Cycler 480 Syber Green I Master Mix (Roche) for cDNA amplification and the qRT-PCR was carried out in a LightCycler 480 II (Roche) for signal detection. RT-PCR results were analyzed using the comparative CT (threshold cycle) method, normalized against the housekeeping gene β-actin.

Immunofluorescence

Detailed description of immunofluorescence is provided in the Supplementary Methods. To evaluate amount of ATP7B in the Golgi, control and treated IGROV or IGROV-CP20 cells cells were immuno-labeled for ATP7B and golgin-97. Golgin 97 staining was used by ROI manager tool of ImageJ software to generate a mask for Golgi region in each cell. The mean pixel intensity of ATP7B signal was measure in the Golgi region of each cell using Measure tool of ImageJ software and reported in arbitrary units (au).

Western blot

Immuno-blotting was performed as described in the Supplementary Methods. Primary antibody against ATP7B, ATP7A, CTR1, GAPDH and α-tunulin were used to detect corresponding proteins.

MTT cell viability assay

Viability of IGROV, IGROV-CP20, A2780, A2780-CP20 and HepG2 cells was determined by measuring their ability to reduce the tetrazolium salt (MTT) to a formazan. The cells were plated in 96-well plate and allowed to adhere overnight. Then the cells were exposed to cisplatin and/or other drugs. After treatment with drugs, the cells were incubated with MTT (Invitrogen). Incubation was stopped using 100 µl of a solution with 25% aqueous ammonia (Sigma) in DMSO (Sigma). Absorbance in each well was recorded at 540 nm in a multi-well plate reader (Synergy/neo, Biotek). The results were normalized to absorbance value in untreated cells (considered to be 100% viable) and expressed as % of viability.

High-throughput screening (HTS)

The overall strategy of HTS is described in the results. For HTS screening, IGROV and IGROV-CP20 cells were plated in 384-well plates. The Prestwick Chemical library of 1280 FDA-approved drugs was screened for compounds that promote cisplatin toxicity in Pt-resistant IGROV-CP20 cells. Triplicates of each drug (at 10µM concentration) were tested alone for 48 h to evaluate own drug toxicity. In parallel set of plates, each drug was used first alone for 24h and then combined with 50µM cisplatin for another 24h. STAR-let liquid handling system (Hamilton) was used to dispense drugs and cisplatin into individual well. Wells containing Pt-sensitive IGROV cells were used as controls to evaluate the extent of cisplatin toxicity. After treatments the viability of cells in the plates was evaluated using MTT assay. The drugs that reduced cell viability only in combination with cisplatin were considered as hits. Overall quality of the screening was controlled through plate uniformity test and correlation between 3 replicates (see Sup Fig. 2).

Metal content determination by inductively coupled plasma mass spectrometry (ICP-MS)

Pt in cell lysates from control and treated cells was analyzed by ICP-MS after wet washing of the samples with nitric acid (Supplementary Methods). Pt concentration was calculated by interpolation under the calibration curve. All values of Pt concentration were normalized for protein content in each specimen. All analyses were performed in triplicates.

DNA adduct evaluation by dot blot

To detect the amount of DNA adducts in control and treated cells, the DNA was extracted from the IGROV-CP20 cells using Quick-DNA Miniprep Plus Kit (Zymo Research). Equal amounts of DNA from each specimen were spotted on a piece of Nytran N nylon blotting membrane (GE Healthcare Life Sciences). Then the membrane was incubated with primary antibody that recognized Pt-induced DNA adducts (Merck, Millipore). The membrane was then washed with TBST incubated with HRP-conjugated secondary antibody according to the manufacturer's instructions. Chemiluminescent signals were captured using Chemidoc Amersham Imager 600 and quantified using ImageJ software.

QuantSeq 3' mRNA and gene ontology enrichment analysis

Three biological replicates of IGROV-CP20 were treated with 50µM cisplatin directly or after 24h incubation with 10µM Tranilast, AmphotericinB or Telmisartan. The impact of each drug on transcriptional response to cisplatin was analyzed using QuantSeq 3' mRNA sequencing. Total RNA was extracted, using the RNeasy Mini Kit (Qiagen, Venlo, Netherlands). RNA extracted from IGROV-CP20 cells treated with cisplatin alone, was used as a control. Total RNA was prepared using QuantSeq 3' mRNA-Seq Library prep kit (Lexogen GmbH, Vienna, Austria) according to the manufacturer's instructions. Amplified cDNA fragments were sequenced in single-end mode using the NextSeq500 (Illumina, San Diego, CA) with a read length of 75 base pairs. Analysis of the sequence reads and Gene Ontology Enrichment Analysis of transcripts is described in the Supplementary Methods.

ATOX-1 trasfection

For transfection, 500 ng/µl of DNA from the Flag-tagged ATOX-1 plasmid (kindly provided from Prof. T. Fukai) was reverse transfected with Opti-MEM and TransIT®-LT1 Transfection Reagent (Mirus Bio LLC, US) according to manufacturer's instructions. Two days after transfection, the cells were pre-treated with Tranilast 0.1 mM for 24 hours and then treated with 50µM cisplatin. After treatments, ATP7B trafficking was analyzed by immunofluorescence and dot immuno-blot analysis was performed to detect the cis-platinum DNA adducts formation. Results shown are from independent transfection experiments, each performed in triplicate.

Wound healing assay

To analyze the impact of cisplatin (or its combination with drugs) on ability of IGROV-CP20 cells to migrate, the cells were seeded in 2 wells culture-insert (Ibidi GmbH, Am Klopferspitz). After the cell attachment, the culture-insert was gently removed and defined 600µm-wide cell-free gap (wound) was generated. The cells were then incubated for 24h with 25µM cisplatin alone or mixed with 10 µM Tranilast, Telmisartan or Amphotericin B. Before wound healing evaluation the cells were washed to remove dead from wounded area and Live/Dead staining was used to ensure absence of dead cells in the remaining wound. The wound closure (cell migration) was monitored using the time-lapse microscopy. Five pictures of the wound at 0, 4, 8, 12, 24-hour time points were captured using ZEISS Axio Observer.Z1 APOTOME. The area of wound was quantified at different time points and % of open wound at 24h of incubation was calculated. The migration rate of IGROV-CP20 cells treated with combination of screening hit drugs and cisplatin was compared with cisplatin treatment alone.

Transwell cell migration assay

IGROV-CP20 cells in serum free RPMI medium were plated on the top of themembrane in a Transwell insert (Cell Biolabs, INC). RPMI with 10% FBS was added to the bottom chamber as desired chemo-attractant. Tranilast, Telmisartan and Amphotorecin B were added to the cells 24 before the transfer to the Transwell insert. Pretreated and control cells were then allowed to migrate through insert membrane in the absence or presence of cisplatin. At the end of incubation the Transwell inserts were fixed, stained with Toloudine Blue and BORAX, and dried.

The inserts were visualized under LEICA M205 FA stereo microscope and the count of the number of cells in different fields of view was performed to get an average of cells that have migrated through the membrane toward the chemo-attractant.

Live/Dead fluorescence cytotoxicity assay

Control and treated IGROV or IGROV-CP20 cells were gently washed with PBS prior to the assay. The Live/Dead reagents (Invitrogen) were combined by adding 10 uL of the 2 mM EthD-1 stock solution and 5 uL of the supplied 4 mM calcein AM stock solution to 10 ml of sterile PBS. Live/Dead solution was added to the cells for 30 minute to generate green fluorescent signal in live cells and red signal in dead cells. The labeled cells were viewed under the fluorescence microscope ZEISS Axio Observer.Z1 APOTOME using FITC and RFP filters to count live cells in the treated and control specimens. Quantification was done in 10 fields for each condition and the proportion of live cells was calculated as % of total cells in the specimen.

Statistical Analysis

Data are expressed as mean ± standard deviation (or SEM), collected from multiple independent experiments performed on different days. Statistical significance for all data, except the QuantSeq and bioinformatics analyses (Supplementary Methods), was computed using Student 2-tailed t tests (for all figures, *P < .05, **P < .01, and ***P < .001 indicate statistical significance).

RESULTS

IGROV-CP20 cells represent a robust system to study ATP7B-mediated cisplatin resistance

Considering that our study was focused on the screening for drugs promoting cisplatin toxicity, we first looked for appropriate cell line to perform HTS. To this end we evaluated response to cisplatin in two ovarian cancer cell lines, IGROV-CP20 and A2780-CP, whose tolerance to Pt drugs has been reported to rely on ATP7B (*10, 29*). Initially, resistance to cisplatin was investigated in the Pt-resistant IGROV-CP20 and in the parental Pt-sensitive IGROV cell lines treated with increasing concentrations of cisplatin (25-100 µM) for 24 and 48 hours. IGROV-

CP20 exhibited significantly higher viability at different cisplatin concentrations than parental IGROV line (Fig.1 A, B). In contrast, the difference in survival of resistant A2780-CP20 and sensitive A2780 cells was less evident (Sup. Fig. 1), indicating IGROV-CP20 line as a more robust cell system for Pt resistance study with HTS. Among tested concentrations, 50 µM cisplatin resulted in the highest difference in survival between IGROV-CP20 and IGROV cells (Fig.1 A, B). Therefore this regimen of cisplatin treatment in IGROV-CP20 cells was further employed for drug screening.

To be sure that ATP7B provides a major contribution to the resistance of IGROV-CP20 cells to cisplatin, we firstly assessed the expression levels of ATP7B. Western blot revealed higher levels of ATP7B, in IGROV-CP20 cells compared to parental IGROV line (Fig. 1C). In parallel, elevated ATP7B expression in IGROV-CP20 line was detected by both RT-qPCR and immunofluorescence (Fig. 1D, E). Finally, ATP7B silencing resulted in two-fold decrease in viability of IGROV-CP20 cells upon cisplatin treatment (Fig. 1F), indicating that Pt-resistance of IGROV-CP20 cells requires ATP7B.

These findings, though, did not allow us to formally rule out that other copper transporters ATP7A or CTR1 may contribute to cisplatin tolerance of IGROV-CP20 cells. Indeed, ICROV-CP20 cells exhibited slightly higher levels of ATP7A protein and mRNA compared to parental cells (Fig. 1G, H). Considering that elevated ATP7A expression confers tolerance to cisplatin in a number of tumors (*9, 13, 30*), we decided to check whether this is a case in IGROV-CP20 cells. However, RNAi-mediated suppression of ATP7A did not result in any decrease in resistance of the cells to cisplatin (Fig. 1I). Next we checked CTR1 expression levels in IGROP-CP20 cells because reduced expression of this transporter has been associated with limited cisplatin uptake and, as a consequence, with higher Pt tolerance (*8, 31*). In contrast with this notion and quite surprisingly, we found that CTR1 expression was higher in IGROV-CP20 cells compared to parental line (Fig. 1J, K). Taken together these findings argue against either ATP7A or CTR1 involvement in cisplatin tolerance in IGROV-CP20 cells line and confirm a key role of ATP7B in Pt resistance mechanism.

Synthetic lethality HTS for FDA-approved drugs revealed positive hits able to promote Pt-mediated death of IGROV-CP20 cells

The strategy of HTS for the detection of FDA approved drugs reducing resistance IGROVCP20 cells to cisplatin was based on the principle of synthetic lethality. A Prestwick Chemical Library of 1280 compounds was dispensed at a concentration of 10 µM in duplicate on the IGROVCP20 cells in the 384 well formats. An MTT calorimetric assay (see Methods) was used as readout for viability of IGROVC-P20 cells upon drug and cisplatin treatments. As shown in heat maps of multi-well plates (Fig.2 A), this assay generated a different degree of MTT signal (encoded in blue color) depending of cell viability, with blue indicating cell survival and white cell death. Parental IGROV cells were used as positive control to test the impact of cisplatin on cell survival and were plated in the first column of the 384 well plates, while the last two columns were left blank as negative control for the assay (Fig. 2A). After the addition of the library compounds, one plate was treated with 50µM of cisplatin for 24h while the other was left without cisplatin to test own toxicity of each drug. This allowed us to exclude the drugs, which were toxic even without cisplatin (Fig. 2A, black boxes), while the drugs promoting cell death only in combination with cisplatin were considered as positive hits (Fig. 2A, red boxes).

Several controls were performed to ensure the assay reproducibility for HTS. Firstly, the assay robustness was estimated by calculating the Z-score factor, which defines the reproducibility and suitability of the assay in full-scale in a high-throughput manner. To this end wells containing IGROV and IGROV-CP20 cells were compared after 24h exposure to cisplatin. Evaluation of MTT signal resulted in Z-score value of 0.279 across the two cell lines thereby indicating a significant difference in viability between sensitive and resistant cells upon cisplatin treatment (Sup. Fig. 2A). This indicates that the difference between response of control IGROV and experimental IGROV-CP20 lines to cisplatin provides a sufficient dynamic range for evaluation of drugs impact during HTS. Secondly, a plate uniformity test was performed to exclude not only any “drift and edge effect” within the plate, but also any systematic source of variability among the samples. Supplementary figure 2B shows that the plates exhibited good uniformity during the screening and no drift and edge effects were detected.

During HTS each component of the library was analyzed in three independent experiments with or without addition of cisplatin. The correlation between 3 replicates was calculated using a Pearson's coefficient that was consistently robust across the experiments (Sup. Fig. 2C), indicating that in each replicate the drugs had a similar impact (as it is desirable for the overall success of HTS screening). Positive hits were identified on the basis of the decrease in cell viability. The arbitrary cut-off threshold for hit detection was set at the level of 5 standard deviations below the average viability of resistant cells in cisplatin (Fig. 2B). Overall, the screening revealed 8 FDA candidates: Clofazimine, Fusidic Acid Sodium salt, Telmisartan, Prochloperazine Dimeleate, Amphotericin B, Tranilast, Roxatidine acetate HCl and Calcipotriene that induced a strong reduction in Pt-resistace of IGROV-CP20 cell (Fig. 2B, C). These compounds were then tested in dose-response experiments, performed using different concentration of each drug (ranging from 0.1 µM to 30 µM) in combination with cisplatin (Fig. 2D; Sup. Fig. 3). The dose-dependent curves showed that some concentrations of tested drugs reduced tolerance of the cells to cisplatin (Sup. Fig. 3). However, only Tranilast, Telmisartan and Amphotericin B exhibited a clear correlation between drug concentration and degree of cell survival in cisplatin (Fig. 2D). Therefore, these 3 drugs were enrolled into further validation.

Validation of hit drug impact on resistance of IGROV-CP20 cells to cisplatin

To validate the efficiency of each HTS hit several assays were employed. Selective live/dead cell staining showed that the toxicity of cisplatin in IGROV-CP20 line was very limited inducing the death barely in 10% of the cells (Fig. 3A, B). However, the level of cell mortality dramatically increased when cisplatin treatment was supplemented with Tranilast, Telmisartant or Amphotericin B (Fig. 3A, B). Among 3 drugs Amphotericin B exhibited the strongest capacity to promote cisplatin toxicity with less than 10% of IRGROV-CP20 cells surviving its combination with cisplatin (Fig. 3A,B). The ability of the hit drugs to promote cisplatin toxicity was also confirmed on other ATP7B-mediated resistant tumor cell line A2780-CP20 (Sup. Fig. 4 A-C), although Amphotorecin B appeared to be quite toxic even alone in this cell type. Interestingly, none of the drugs was able to further increase Pt-mediated death in sensitive IGROV cells (Sup. Fig. 4D).

At this point it was intriguing to verify a potential of each drugs to promote the formation of *cis*-platinum DNA adducts in the resistant cells. To this end we employed dot immuno-blot assay with a specific antibody capable of recognizing DNA adducts (see Methods). After cisplatin treatment Pt-sensitive IGROV cells exhibited significantly higher adduct-associated signal compared to the resistant IGROV-CP20 cells (Figure 3C, D). Addition of hit drugs in combination with cisplatin significantly increased the adducts signal of spotted DNA compared to cisplatin alone (Figure 3 C, D) even thought only Amphotorecin B elevated overall intracellular levels of Pt (Fig. 3E). Moreover, the drugs increased the abundance of adduct in IGROV-CP20 cells to the levels similar to those observed in Pt-sensitive parental cell line (Fig. 3C, D), thereby indicating a significant potential of hit drugs to promote Pt-mediated damage of DNA in resistant cells.

Since each of the three FDA-approved molecules stimulated Pt-induced cell death, we tested their capacity to affects cell migration, which is usually considered to be feature of tumor cell invasiveness. Figures 4A and B shows that combination of Tranilast and Telmisartan with cisplatin significantly slowed the rate of IGROV-CP20 cells migration through Transwell membrane, while cisplatin alone did not impact cell migration. Furthermore, the combination of cisplatin with either Tranilast or Telmisartan significantly reduced ability of IGROV-CP20 cells to repopulate wounded area (Fig. 4C, D). Control experiments revealed that resistant tumor sealed more than 80% of the open wound after 24h, whereas cisplatin slightly attenuated wound healing. In contrast, combination of cisplatin with Tranilast and Telmisartan caused a marked inhibition of the migration into wound area over the same time period (Fig.4 C, D). It worth noting that combination of cisplatin with even low concentrations Amphotorecin B was so toxic that we did not get sufficient starting cell material to perform either Transwell invasion or wound healing assays.

Finally, the impact of all 3 hits on Pt accumulation was investigated using ICP-MS. In control experiments we found that exposure of sensitive IGROV cells to cisplatin resulted in a significant increase in the intracellular Pt levels, while Pt remained scarce in the resistant IGROV-CP20 cells even after 24h incubation with cisplatin. Interestingly, among 3 hit drugs only Amphotericin B induced a significant accumulation of Pt in IGROV-CP20 cells, while the addition

of Tranilast or Telmisartan in combination with cisplatin did not cause any significant increase in Pt levels (Fig.3 E). This prompted us to further investigate the mechanism through which Tranilast, Telmisartant and Amphotericin B amplify the sensitivity of resistant tumor cells to cisplatin.

FDA-approved hit drugs affect ATP7B trafficking in Pt-resistant tumor cells

Considering that none of the hit drugs caused reduction in ATP7B expression (see below), we examined the intracellular localization of ATP7B in IGROV-CP20 cells. We found that addition of cisplatin predictably stimulated exit of ATP7B from the Golgi (Fig.4A), as this process is apparently required for proper metal sequestration/efflux (*10, 32*). However, pretreatment of IGROV-CP20 cells with Tranilast, Telmisartant or Amphotericin B was able to inhibit ATP7B Pt-mediated export from the Golgi (Fig.4 A, B). This was particularly evident for Tranilast and Telmisartan treatments, in which a significant increase in ATP7B retention in the Golgi region was detected (Fig 4B). These results were intriguing since they suggest that these drugs could have an impact on ATP7B trafficking, thereby inducing cisplatin accumulation within the cells and subsequent tumor cell death.

However, in the context of eventual clinical use, the inhibitory impact of these drugs on ATP7B trafficking might present a risk of toxic copper accumulation in the liver where ATP7B trafficking is needed for sequestration of excess copper and its further efflux to the bile (*17, 18*). Therefore, we tested whether Tranilast, Telmisartan or Amphotericin B alter copper-dependent ATP7B trafficking in hepatic HepG2 cells. Luckily, none of the drugs inhibited copper-induced export of ATP7B from the Golgi (Sup. Fig.5 A,B). In line with no impact on ATP7B trafficking, all 3 drugs failed to stimulate cisplatin toxicity in HepG2 cells (Sup. Fig. 5C) indicating that these drugs act though a mechanism that is likely to be specific for Pt-resitant ovarian tumor cells.

Hits drugs affect expression of genes operating in different Pt-resistance pathways

Considering that cisplatin tolerance usually relies on several different mechanisms even in the single cell type, we sought to investigate whether Tranilast, Telmisartan or Amphotericin B affect Pt-resistance pathways that does not involve ATP7B. To verify this a QuantSeq mRNA technology was employed to analyze global transcriptional response to each drug. Likewise

QRT-PCR, QuantSeq 3' mRNA sequencing allows very accurate measurements of quantitative difference in gene expression (*33*). The advantage of this technology consists in simultaneous and rapid analysis of entire transcriptome, while QRT-PCR is usually limited to subsets of dozens genes at best (*33*).

Thus, gene expression values in IGROV-CP20 cells, which were treated with cisplatin alone, were compared to those in the cells treated with combination of cisplatin and each hit drug. QuantSeq analysis revealed all 3 drugs to modulate gene expression in cisplatin-treated cells (Figure 5C). Amphotericin B induced 1452 and suppressed 1854 genes, while Tranilast treatment resulted in 2164 up-regulated and 1786 down-regulated genes compared to cells treated with cisplatin alone (Figure 5C). In contrast, Telmisartan induced transcriptional changes in a quite limited cohort of genes (Figure 5C). We noted that none of the drugs decreased the levels of ATP7B mRNA (see supplementary data).

To determine the biological pathways affected by drugs in cisplatin-treated cells, gene ontology (GO) enrichments were calculated (see Methods). GO analysis of Tranilast- and Amphotericin B-treated cells revealed several statistically significant GO enrichments that exhibited a similar trend in several groups of down-regulated genes (Figure 5D). These include DNA repair; protein quality control, ubiquitination and folding; macroautophagy and NFKB signaling, which all were reported to promote cisplatin resistance (*25-27, 34*). Overall, among a total of 19 significant GO biological clusters identified in the down-regulated genes, 4 pathways were found in common between Amphotericin B and Tranilast (Figure 5D). Surprisingly, only Tranilast-treated samples displayed a significant down-regulation of genes involved in copper ion binding (Figure 5D). This finding was intriguing because it could possibly explain the enhanced cell lethality in the case of Tranilast treatment. Indeed, this cohort of genes comprised ATOX1, COX17 and SOD1 (Fig. 6A), involved in copper and platinum distribution toward different cellular destinations such as secretory system, mitochondria and free radical detoxification pathway, respectively (*35-39*). Thus, by affecting ATOX1, COX17 and SOD1, Tranilast might inhibit delivery Pt to this pathways, thereby favoring its transport to the cell nuclei, where Pt promotes DNA damage resulting in cell death (Fig. 6B).

Tranilast affects ATP7B trafficking in Pt-resistant tumor cells via down-regulation of ATOX1

Among the copper-binding genes, which were down-regulated by Tranilast, we decided to focus on *ATOX1*. Previous literature data reported that some Pt-resistant cells express higher levels of ATOX1, which facilitate transfer of active cisplatin to ATP7B (*40*), thereby promoting Pt resistance. Moreover, *ATOX1* silencing has been associated to a reduced invasiveness of breast cancer cells (*41*) thereby supporting the potential of Tranilast suppress viability and migration of resistant tumor cells. Notably, we did not find any significant impact of either cisplatin or Tranilast on ATOX1 expression in hepatic HepG2 cells (Sup. Fig. 5D), indicating that ATOX1 might be targeted by Tranilast in a safe tumor-specific manner. Therefore, we sought to investigate whether overexpression of ATOX1 is able to overcome Tranilast impact by recovering (at least partially) the resistance of IGROV-CP20 cells to cisplatin. We also considered this analysis as a proof of principle experiment to verify whether transcriptomics provides really meaningful information regarding hit drug action mechanisms.

We reasoned that overexpressing exogenous ATOX1 under generic CMV promoter should allow IGROV-CP20 cells to circumvent inhibitory impact of Tranilast on transcription of endogenous ATOX1. Thus the cells were transfected with ATOX1-FLAG plasmid (*42*) and incubated with cisplatin alone or in combination with Tranilast. Initially we analyzed the impact of ATOX1 overexpression on Pt-dependent trafficking of ATP7B in Tranilast-treated cells. Confocal microscopy revealed that ATOX1-overexpressing cells supported Pt-induced relocation of ATP7B from the Golgi to cell periphery even in the presence of Tranilast (Fig. 6C). In contrast, Tranilast still inhibited Pt-dependent export of ATP7B from the Golgi in the cells that did not overexpress ATOX1 (Fig. 6C). Correspondingly, MTT viability assay confirmed that the overexpression of ATOX1 blocked ability of Tranilast to promote cisplatin toxicity in IGROV-CP20 cells (Fig. 6D). Furthermore, dot blot experiments revealed that ATOX1 overexpression significantly reduced capacity of Tranilast to induce formation of DNA-platinum adducts (Figure 5E). These findings indicate that ATOX1 contributes to cisplatin resistance in ovarian cancer cells, while its down-regulation with Tranilast promotes Pt-mediated cell death.

DISCUSSION

Resistance of tumors to chemotherapy represents an important challenge in modern oncology. Although Pt-based drugs demonstrated excellent therapeutic potential their effectiveness in wide range of tumors is limited by development of resistance mechanisms including increased Pt sequestration/efflux by ATP7B (*1, 6, 7*). In this context ATP7B emerges as an attractive target to combat Pt resistance. Indeed, silencing ATP7B has been demonstrated to reduce tolerance of tumor cells to Pt-based drugs in vitro and in vivo (*29*). However the ATP7B RNAi strategy has been never advanced to therapy due to potential risks of compromising Cu homeostasis in patients. Considering that ATP7B suppression leads to rapid accumulation of hepatic copper and liver damage (*17*), ATP7B-activity in Pt-resistant tumors should be targeted in a selective manner or circumvented in a safe manner to avoid hepatic complications. In this context, we reasoned that identification of the bio-safe FDA/EMA-approved drugs might help to achieve this objective.

Here using synthetic lethality screening we detected and validated three FDA-approved drugs Tranilast, Telmisartan and Amphotericin B, which overcome ATP7B-mediated resistance in ovarian cancer cells. All 3 drugs promoted cisplatin-mediated death via stimulation of Pt-DNA adduct formation. As a consequence, cell growth and migration were seriously compromised indicating a significant reduction in tumorigenic potential of IGROV-CP20 cells. Notably, the efficiency of Tranilast, Telmisartan and Amphotericin B was confirmed in another cisplatin-resistant ovarian cancer A2870-CP20 cell line. However, the hit drugs did not enhance cisplatin toxicity in parental Pt-sensitive IGROV cells supporting the notion that resistant cells develop specific tolerance mechanisms (*1, 43*) that might be targeted in a selective manner.

Despite the similar impact, the hit drugs exhibited a clear difference in their ability to promote accumulation of platinum in resistant cells. Only Amphotericin B treatment resulted in a significant increase in intracellular Pt levels but how remains unclear. RNA-seq data suggest that the drug did not induce changes in expression of copper transporters that would favor copper accumulation. Probably Amphotericin B binding to the membrane sterol lipids might modulate permeability of the cell surface transporters or even cause physical damage of the membrane favoring elevated uptake of cisplatin (*44*).

In contrast to Amphotericin B, Tranilast and Telmisartan did not accelerate Pt accumulation but still were able to facilitate DNA adduct formation. Thus, it is tempting to hypothesize that both drugs affect the cellular fluxes of Pt thereby favoring delivery of the metal to the nucleus. Indeed, both Tranilast and Telmisartan inhibited export of ATP7B from the Golgi in response to cisplatin. This trafficking event is apparently needed for delivery of ATP7B to the lumen of peripheral endo-lysosomal structures (*20, 45*), where reduced pH favors metal-transporting activity of ATP7B (*46*). This in turn leads to sequestration of Pt to the lumen of these organelles and its further detoxification (*3*). Therefore, failure of ATP7B trafficking in Tranilast- and Telmisartan-treated cells favors toxic accumulation of Pt in other cells compartment and increases its chances to arrive to the nucleus and damage the DNA. Interestingly, some ATP7B retention was also observed in the case of Amphotorecin B treatment of ICROV-CP20 cells but at lower degree then it was observed for other hit drugs.

The mechanisms through which the hit drugs inhibit ATP7B trafficking remains unclear except for Tranilast, which reduce ATOX1 expression in resistant tumor cells. Elevated expression of ATOX1 was associated with tolerance to cisplatin in several tumor cell lines (*40*). ATOX1 operates as a specific chaperon, which ferries incoming Cu or Pt to ATP7B thereby stimulating metal-dependent trafficking of ATP7B (*38*). Tranilast-mediated suppression of ATOX1 apparently reduces supply of Pt to ATP7B thereby inhibiting its trafficking to post-Golgi compartments operating in Pt sequestration/efflux. In line with our observations, silencing of ATOX1 has been reported to reduce tolerance to cisplatin in tumor cells (*47*). Importantly, we found that Tranilast affected neither ATOX1 expression, nor ATP7B trafficking, nor cisplatin toxicity in hepatic cells, where ATP7B is required to maintain Cu homeostasis. This indicates that Tranilast targets ATP7B-mediated resistance mechanism in a tumor-specific manner, which strongly reduces a risk of side effects and adverse events upon therapeutic use.

Although ATP7B expression and trafficking provided a significant contribution to cisplatin tolerance in tested ovarian cancer cells, it is likely that other mechanisms are involved in Pt-resistance because usually cisplatin treatment cause complex and multifactorial cellular responses (*6*). To understand whether and how FDA-approved hit drugs affect such responses of tumor cells to cisplatin we used systems biology approach and investigated drug-induced

changes in transcriptome. Notably, copper transporters CTR1, ATP7A and ATP7B did not manifest the changes in expression, which would favor Pt toxicity in drug-treated cells. However, GO analysis revealed that transcriptional response to Tranilast and Amphotericin B shares suppression of several cisplatin resistance pathways including DNA repair (*28*), anti-apoptotic NFKB signaling (*25*) and protein quality control (*27*). In addition to these mechanisms, we noted that both drugs reduced expression of autophagy genes. Autophagy has recently emerged as important mechanisms for Cu and Pt detoxification (*26, 48*) and its role in resistance of tumor cells to cisplatin was documented (*49, 50*). Therefore, the example of Tranilast and Amphotericin B suggests that autophagy might be targeted for reduction of tumor tolerance to Pt-based drugs.

However the impact of Tranilast on transcriptional response of resistant cells to cisplatin exhibited a particular feature that consisted in down-regulation of numerous genes regulating Cu metabolism. This finding was of particular interest because Cu and Pt are frequently handled by the same intracellular pathways that also operate in cisplatin resistance (*4, 32, 51*). The cohort of Tranilast-sensitive transcripts included ATOX1, COX17 and SOD1 that normally supply Cu to biosynthetic, mitochondrial and anti-oxidant pathways, respectively (*17*). Pt binding to ATOX1, COX17 and SOD1 was documented (*52-55*), moreover increase in SOD1 and ATOX1 expression has been suggested to confer cisplatin resistance to tumor cells (*40, 52, 56*). Thus, reduced expression of these three genes in Tranilast-treated cells should result in increased amounts of Pt directed towards other cellular destinations comprising nucleus and DNA (see scheme in Fig. 6B). Indeed, we found that Tranilast treatment strongly promoted Pt-induced DNA damage in resistant tumor cells. Suppression of ATOX1 might also help to combat tumor growth through additional mechanisms. As mentioned above ATOX1 deficit inhibits ATP7B trafficking and hence its ability to sequester/efflux toxic Pt. Moreover, ATOX1 activity stimulates angiogenesis (*42*). Considering that vascularization of tumors support their survival and growth, Tranilast might inhibit these processes counteracting ATOX1-mediated angiogenesis.

Regardless mechanistic similarities and differences between all three identified FDA-approved drugs, they share a number of clinically important features. Firstly, they efficiently circumvent

ATP7B resistance in ovarian cancer cells. Thus, considering known biosafety profiles of these drugs, their translation to clinical use might be relatively rapid. Tranilast inhibits the production of interleukin-6 and is normally used as anti-allergic drug, which is well tolerated by most patients at very substantial doses (*57*). Telmisartan also appears to be a quite safe agent. It operates as angiotensin II receptor antagonist to treat hypertension (*58, 59*). Amphotericin B is antifungal drug and appears to be less safe among 3 hits due to nephrotoxicity (*60*), although some strategies to reduce its toxicity were recently developed (*61*). Interestingly, Tranilast and Amphotericin B were reported to promote Pt toxicity in a number of tumor cell lines including mesothelioma, oral squamous carcinoma and gastric cancer (*60, 62-64*). Therefore their use might be expanded beyond ovarian cancer. Secondly, all three hit drugs did not potentiate cisplatin toxicity in parental ovarian cancer cells, which do not manifest any significant resistance to Pt-based drugs. This indicates that combination of Tranilast, Telmisartan and Amphotericin B with cisplatin should be employed only to treat resistant tumors, while use of these drugs would be worthless in patients, which efficiently respond to cisplatin therapy. Finally, despite the ability to suppress Pt-resistance mechanisms including ATP7B trafficking, all 3 drugs did not stimulate Pt toxicity in hepatic cells. This indicates that the drugs target tumor-specific mechanisms of cisplatin resistance in a highly selective manner and, hence, do not pose any significant risk of promoting Pt toxicity or compromising Cu homeostasis in the liver, thereby, reducing the risks of adverse events in eventual clinical use.

In conclusion, our study demonstrates that HTS emerges as an effective approach that might be used to detect candidate drugs for repurposing in oncologic use. Using this strategy we revealed FDA-approved drugs that overcome ATP7B-madiated resistance to cisplatin in ovarian cancer cells and characterized several molecular mechanisms behind the drug impacts. We believe that identification of these drugs will help to accelerate development of new strategies to combat cancer resistance to cisplatin therapy, which still represents an important challenge in modern oncology

ACKNOWLEDGMENTS

This work was supported by AIRC, Italy (Grant #IG 17118 to RSP); Telethon, Italy (Grant #TIGEM-CBDM9 to RSP) and Veronesi Foundation, Italy (Fellowship to RP). We also acknowledge support from TIGEM bioinformatics, NGS, HCS and microscopy cores.

REFERENCES

1. Z. H. Siddik, Cisplatin: mode of cytotoxic action and molecular basis of resistance. *Oncogene* **22**, (2003).
2. T. Boulikas, M. Vougiouka, Cisplatin and platinum drugs at the molecular level. (Review). *Oncol Rep* **10**, 1663-1682 (2003).
3. R. Safaei *et al.*, Abnormal lysosomal trafficking and enhanced exosomal export of cisplatin in drug-resistant human ovarian carcinoma cells. *Mol Cancer Ther* **4**, (2005).
4. M. T. Kuo, S. Fu, N. Savaraj, H. H. Chen, Role of the human high-affinity copper transporter in copper homeostasis regulation and cisplatin sensitivity in cancer chemotherapy. *Cancer Res* **72**, 4616-4621 (2012).
5. T. Gupta *et al.*, Radical radiotherapy with concurrent weekly cisplatin in loco-regionally advanced squamous cell carcinoma of the head and neck: a single-institution experience. *Head Neck Oncol* **1**, 17 (2009).
6. L. Galluzzi *et al.*, Molecular mechanisms of cisplatin resistance. *Oncogene* **31**, 1869-1883 (2012).
7. J. Helleman *et al.*, Impaired cisplatin influx in an A2780 mutant cell line: evidence for a putative, cis-configuration-specific, platinum influx transporter. *Cancer Biol Ther* **5**, 943-949 (2006).
8. S. Ishida, J. Lee, D. J. Thiele, I. Herskowitz, Uptake of the anticancer drug cisplatin mediated by the copper transporter Ctr1 in yeast and mammals. *Proc Natl Acad Sci U S A* **99**, 14298-14302 (2002).
9. R. Safaei, A. K. Holzer, K. Katano, G. Samimi, S. B. Howell, The role of copper transporters in the development of resistance to Pt drugs. *J Inorg Biochem* **98**, (2004).
10. R. Safaei, S. B. Howell, Copper transporters regulate the cellular pharmacology and sensitivity to Pt drugs. *Crit Rev Oncol Hematol* **53**, (2005).
11. M. Komatsu *et al.*, Copper-transporting P-type adenosine triphosphatase (ATP7B) is associated with cisplatin resistance. *Cancer Res* **60**, (2000).
12. R. Safaei, S. B. Howell, in *Cancer Drug Resistance,* B. A. Teicher, Ed. (Humana Press, Totowa, NJ, 2006), pp. 309-327.
13. G. Samimi *et al.*, Increased expression of the copper efflux transporter ATP7A mediates resistance to cisplatin, carboplatin, and oxaliplatin in ovarian cancer cells. *Clin Cancer Res* **10**, (2004).
14. Z. H. Li *et al.*, Copper-transporting P-type adenosine triphosphatase (ATP7A) is associated with platinum-resistance in non-small cell lung cancer (NSCLC). *J Transl Med* **10**, 21 (2012).
15. E. V. Polishchuk *et al.*, Wilson disease protein ATP7B utilizes lysosomal exocytosis to maintain copper homeostasis. *Dev Cell* **29**, 686-700 (2014).
16. E. V. Polishchuk, R. S. Polishchuk, The emerging role of lysosomes in copper homeostasis. *Metallomics* **8**, 853-862 (2016).
17. S. Lutsenko, N. L. Barnes, M. Y. Bartee, O. Y. Dmitriev, Function and regulation of human copper-transporting ATPases. *Physiol Rev* **87**, 1011-1046 (2007).
18. S. La Fontaine, J. F. Mercer, Trafficking of the copper-ATPases, ATP7A and ATP7B: role in copper homeostasis. *Arch Biochem Biophys* **463**, 149-167 (2007).
19. F. Tadini-Buoninsegni *et al.*, Translocation of platinum anticancer drugs by human copper ATPases ATP7A and ATP7B. *Angew Chem Int Ed Engl* **53**, 1297-1301 (2014).
20. G. V. Kalayda, C. H. Wagner, I. Buß, J. Reedijk, U. Jaehde, Altered localisation of the copper efflux transporters ATP7A and ATP7B associated with cisplatin resistance in human ovarian carcinoma cells. *BMC Cancer* **8**, 175 (2008).

21. K. Katano *et al.*, Confocal microscopic analysis of the interaction between cisplatin and the copper transporter ATP7B in human ovarian carcinoma cells. *Clin Cancer Res* **10**, (2004).
22. N. V. Dolgova, D. Olson, S. Lutsenko, O. Y. Dmitriev, The soluble metal-binding domain of the copper transporter ATP7B binds and detoxifies cisplatin. *Biochem J* **419**, 51-56, 53 p following 56 (2009).
23. R. Safaei, P. L. Adams, M. H. Maktabi, R. A. Mathews, S. B. Howell, The CXXC motifs in the metal binding domains are required for ATP7B to mediate resistance to cisplatin. *J Inorg Biochem* **110**, 8-17 (2012).
24. T. T. Ashburn, K. B. Thor, Drug repositioning: identifying and developing new uses for existing drugs. *Nat Rev Drug Discov* **3**, 673-683 (2004).
25. B. Thakur, P. Ray, Cisplatin triggers cancer stem cell enrichment in platinum-resistant cells through NF-kappaB-TNFalpha-PIK3CA loop. *J Exp Clin Cancer Res* **36**, 164 (2017).
26. W. J. Buchser, T. C. Laskow, P. J. Pavlik, H. M. Lin, M. T. Lotze, Cell-mediated autophagy promotes cancer cell survival. *Cancer Res* **72**, 2970-2979 (2012).
27. H. W. Moon, H. G. Han, Y. J. Jeon, Protein Quality Control in the Endoplasmic Reticulum and Cancer. *Int J Mol Sci* **19**, (2018).
28. B. Koberle, M. T. Tomicic, S. Usanova, B. Kaina, Cisplatin resistance: preclinical findings and clinical implications. *Biochim Biophys Acta* **1806**, 172-182 (2010).
29. L. S. Mangala *et al.*, Therapeutic Targeting of ATP7B in Ovarian Carcinoma. *Clin Cancer Res* **15**, 3770-3780 (2009).
30. K. Katano *et al.*, Acquisition of resistance to cisplatin is accompanied by changes in the cellular pharmacology of copper. *Cancer Res* **62**, 6559-6565 (2002).
31. X. Lin, T. Okuda, A. Holzer, S. B. Howell, The copper transporter CTR1 regulates cisplatin uptake in Saccharomyces cerevisiae. *Mol Pharmacol* **62**, 1154-1159 (2002).
32. R. Safaei, Role of copper transporters in the uptake and efflux of platinum containing drugs. *Cancer Lett* **234**, (2006).
33. P. Moll, M. Ante, A. Seitz, T. Reda, QuantSeq 3[prime] mRNA sequencing for RNA quantification. *Nat Meth* **11**, (2014).
34. S. Shukla, S. Gupta, Suppression of constitutive and tumor necrosis factor alpha-induced nuclear factor (NF)-kappaB activation and induction of apoptosis by apigenin in human prostate carcinoma PC-3 cells: correlation with down-regulation of NF-kappaB-responsive genes. *Clin Cancer Res* **10**, 3169-3178 (2004).
35. V. C. Culotta *et al.*, The copper chaperone for superoxide dismutase. *J Biol Chem* **272**, 23469-23472 (1997).
36. P. C. Wong *et al.*, Copper chaperone for superoxide dismutase is essential to activate mammalian Cu/Zn superoxide dismutase. *Proc Natl Acad Sci U S A* **97**, 2886-2891 (2000).
37. I. Hamza, J. Prohaska, J. D. Gitlin, Essential role for Atox1 in the copper-mediated intracellular trafficking of the Menkes ATPase. *Proc Natl Acad Sci U S A* **100**, 1215-1220 (2003).
38. I. Hamza, M. Schaefer, L. W. Klomp, J. D. Gitlin, Interaction of the copper chaperone HAH1 with the Wilson disease protein is essential for copper homeostasis. *Proc Natl Acad Sci U S A* **96**, 13363-13368 (1999).
39. R. Amaravadi, D. M. Glerum, A. Tzagoloff, Isolation of a cDNA encoding the human homolog of COX17, a yeast gene essential for mitochondrial copper recruitment. *Hum Genet* **99**, 329-333 (1997).
40. M. E. Palm *et al.*, Cisplatin binds human copper chaperone Atox1 and promotes unfolding in vitro. *Proc Natl Acad Sci U S A* **108**, 6951-6956 (2011).
41. S. Blockhuys, P. Wittung-Stafshede, Copper chaperone Atox1 plays role in breast cancer cell migration. *Biochem Biophys Res Commun* **483**, 301-304 (2017).
42. A. Das *et al.*, Endothelial Antioxidant-1: a Key Mediator of Copper-dependent Wound Healing in vivo. *Sci Rep* **6**, 33783 (2016).
43. Y. Y. Lee *et al.*, Prognostic value of the copper transporters, CTR1 and CTR2, in patients with ovarian carcinoma receiving platinum-based chemotherapy. *Gynecol Oncol* **122**, 361-365 (2011).
44. L. Poulain *et al.*, Potentiation of cisplatin and carboplatin cytotoxicity by amphotericin B in different human ovarian carcinoma and malignant peritoneal mesothelioma cells. *Cancer Chemother Pharmacol* **40**, 385-390 (1997).
45. K. Katano *et al.*, The copper export pump ATP7B modulates the cellular pharmacology of carboplatin in ovarian carcinoma cells. *Mol Pharmacol* **64**, 466-473 (2003).

46. R. Safaei, S. Otani, B. J. Larson, M. L. Rasmussen, S. B. Howell, Transport of cisplatin by the copper efflux transporter ATP7B. *Mol Pharmacol* **73**, 461-468 (2008).
47. R. Safaei, M. H. Maktabi, B. G. Blair, C. A. Larson, S. B. Howell, Effects of the loss of Atox1 on the cellular pharmacology of cisplatin. *J Inorg Biochem* **103**, 333-341 (2009).
48. E. V. Polishchuk *et al.*, Activation of Autophagy, Observed in Liver Tissues From Patients With Wilson Disease and From Atp7b-Deficient Animals, Protects Hepatocytes From Copper-Induced Apoptosis. *Gastroenterology*, (2018).
49. L. Bao *et al.*, Induction of autophagy contributes to cisplatin resistance in human ovarian cancer cells. *Mol Med Rep* **11**, 91-98 (2015).
50. X. Sui *et al.*, Autophagy and chemotherapy resistance: a promising therapeutic target for cancer treatment. *Cell Death Dis* **4**, e838 (2013).
51. S. B. Howell, R. Safaei, C. A. Larson, M. J. Sailor, Copper transporters and the cellular pharmacology of the platinum-containing cancer drugs. *Mol Pharmacol* **77**, 887-894 (2010).
52. M. E. Palm-Espling, C. Lundin, E. Bjorn, P. Naredi, P. Wittung-Stafshede, Interaction between the anticancer drug Cisplatin and the copper chaperone Atox1 in human melanoma cells. *Protein Pept Lett* **21**, 63-68 (2014).
53. V. Calandrini *et al.*, Structural biology of cisplatin complexes with cellular targets: the adduct with human copper chaperone atox1 in aqueous solution. *Chemistry* **20**, 11719-11725 (2014).
54. L. Zhao *et al.*, Cisplatin binds to human copper chaperone Cox17: the mechanistic implication of drug delivery to mitochondria. *Chem Commun (Camb)* **50**, 2667-2669 (2014).
55. L. Banci *et al.*, Interaction of cisplatin with human superoxide dismutase. *J Am Chem Soc* **134**, 7009-7014 (2012).
56. D. P. Brown, H. Chin-Sinex, B. Nie, M. S. Mendonca, M. Wang, Targeting superoxide dismutase 1 to overcome cisplatin resistance in human ovarian cancer. *Cancer Chemother Pharmacol* **63**, 723-730 (2009).
57. S. Darakhshan, A. Ghanbari, F. Gholami Rad, A. Bidmeshki Pour, Tamoxifen and tranilast show a synergistic effect against breast cancer in vitro. *Bratisl Lek Listy* **116**, 69-73 (2015).
58. H. Kakuta, K. Sudoh, M. Sasamata, S. Yamagishi, Telmisartan has the strongest binding affinity to angiotensin II type 1 receptor: comparison with other angiotensin II type 1 receptor blockers. *Int J Clin Pharmacol Res* **25**, 41-46 (2005).
59. D. Galzerano *et al.*, Three-dimensional echocardiographic and magnetic resonance assessment of the effect of telmisartan compared with carvedilol on left ventricular mass a multicenter, randomized, longitudinal study. *Am J Hypertens* **18**, 1563-1569 (2005).
60. P. Bergstrom, A. Johnsson, E. Cavallin-Stahl, T. Bergenheim, R. Henriksson, Effects of cisplatin and amphotericin B on DNA adduct formation and toxicity in malignant glioma and normal tissues in rat. *Eur J Cancer* **33**, 153-159 (1997).
61. G. P. Patel, C. W. Crank, J. B. Leikin, An evaluation of hepatotoxicity and nephrotoxicity of liposomal amphotericin B (L-AMB). *J Med Toxicol* **7**, 12-15 (2011).
62. K. Murahashi *et al.*, Tranilast and cisplatin as an experimental combination therapy for scirrhous gastric cancer. *Int J Oncol* **13**, 1235-1240 (1998).
63. N. Noguchi, S. Kawashiri, A. Tanaka, K. Kato, H. Nakaya, Effects of fibroblast growth inhibitor on proliferation and metastasis of oral squamous cell carcinoma. *Oral Oncol* **39**, 240-247 (2003).
64. T. Morikage *et al.*, Reversal of cisplatin resistance with amphotericin B in a non-small cell lung cancer cell line. *Jpn J Cancer Res* **82**, 747-751 (1991).

Figure 1

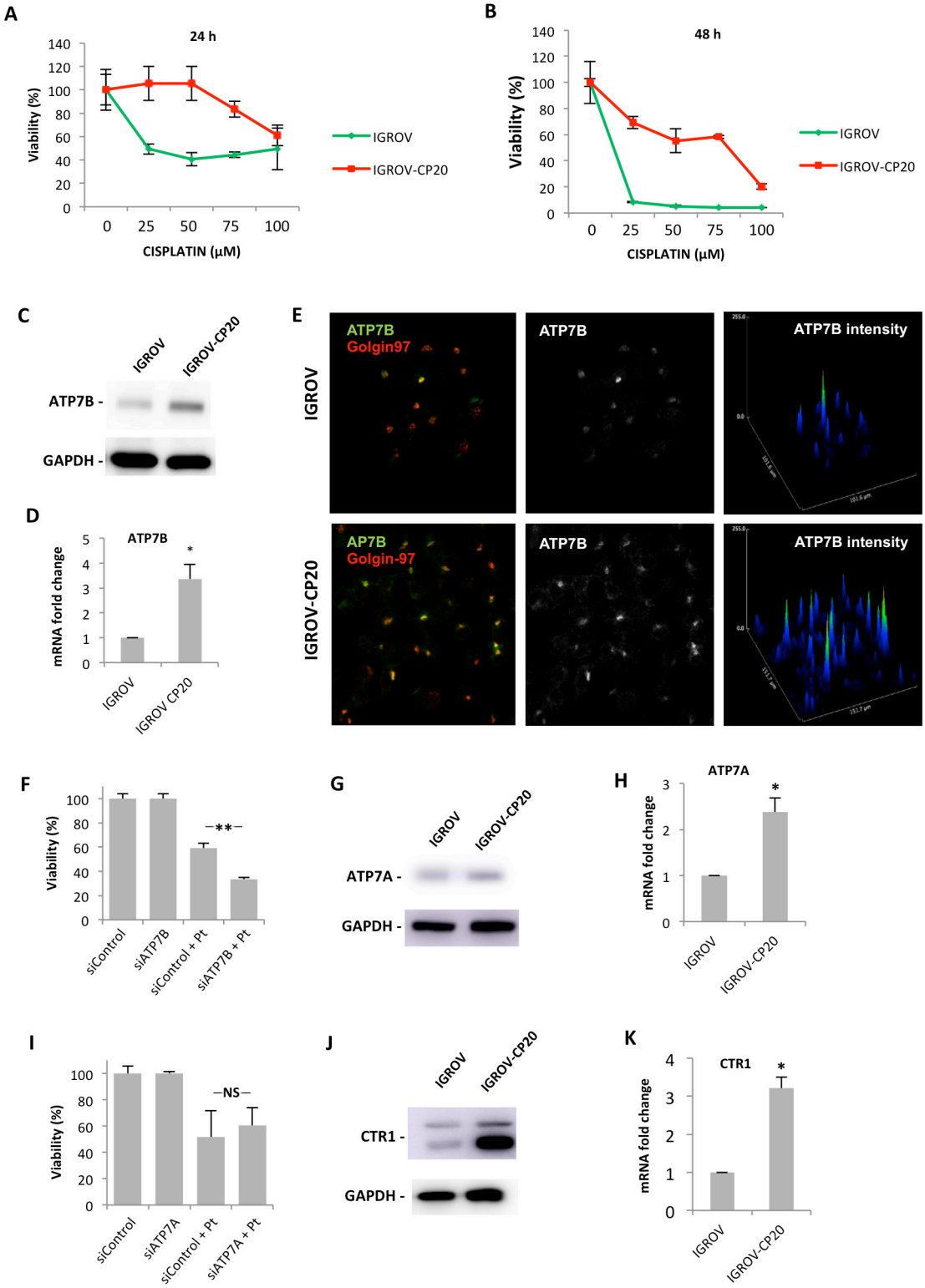

Figure 1. **Cisplatin resistance** of **IGROV-CP20 cells requires ATP7B.**
(A, B) IGROV (green line) and IGROV-CP20 (red line) cells were treated with indicated concentrations of cisplatin for 24 **(A)** and 48 h **(B)** and viability of the cells was then evaluated using MTT assay. **(C)** Western Blot revealed higher levels of ATP7B protein in IGROV-CP20 cells compared to the parental IGROV cell line. **(D)** qRP-PCR revealed higher mRNA levels of ATP7B in resistant IGROV-CP20 cells then in sensitive IROV cells (n=3 experiments; *p<0.05, t-test). **(E)** IGROV and IGROV-CP20 cells were labeled for endogenous ATP7B and Golgin-97. Graphs (right column) indicate higher levels of ATP7B signal in IGROV-CP20 cells respect to parental line. The plots were generated using Zen 2012 software at LSM-700 Zeiss confocal microscope. **(F)** IGROV-CP20 cells were transfected with control (siControl) or ATP7B-specific siRNAs and incubated with 50µM cisplatin. MTT assay indicated reduced tolerance to cisplatin in ATP7B-silenced cells (n=3 experiments; **p<0.01, t-test). **(G)** Western Blot revealed slightly higher levels of ATP7A protein in IGROV-CP20 cells compared to the parental IGROV cell line. **(H)** qRP-PCR revealed higher mRNA levels of ATP7B in resistant IGROV-CP20 cells then in sensitive IROV cells (n=3 experiments; *p<0.05, t-test). **(I)** IGROV-CP20 cells were transfected with control (siControl) or ATP7A-specific siRNAs and incubated with 50µM cisplatin. MTT assay did not detect viability differences between cisplatin treated control and ATP7A-silenced cells. **(J)** Western Blot revealed higher levels of CTR1 in IGROV-CP20 cells compared to the parental IGROV cell line. **(K)** qRP-PCR detected higher mRNA levels of CTR1 in resistant IGROV-CP20 cells then in sensitive IROV cells (n=3 experiments; *p<0.05, t-test).

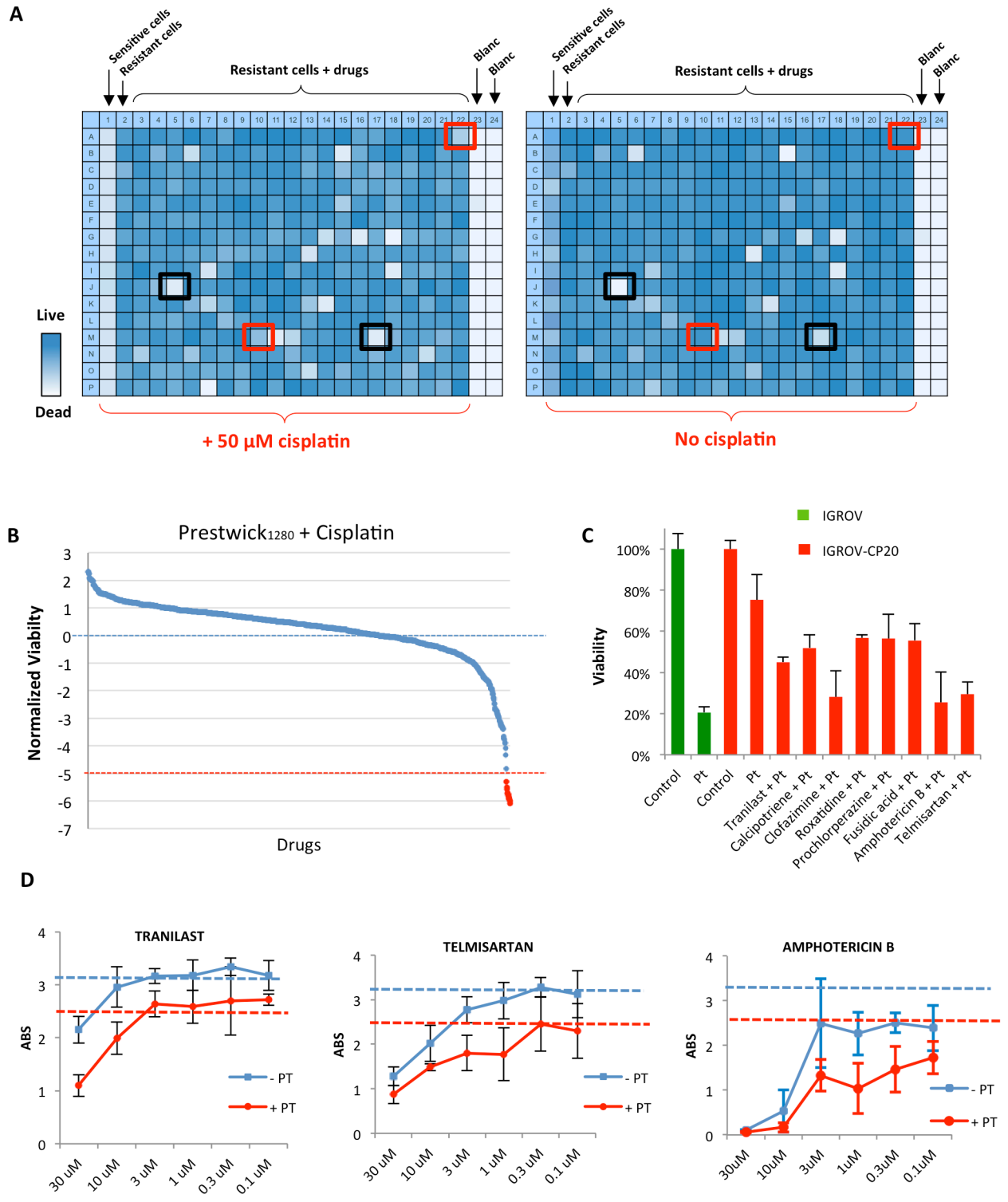

Figure 2: Synthetic lethality screening revealed FDA-approved drugs that promote Pt-mediated death of IGROV-CP20 cells
(A) Real heat maps showing MTT signal in two 384 well plates from the HCS screening. Sensitive IGROV cells were used as negative control while IGROV-CP20 cells were seeded in central areas of each plate and treated with drugs from a library of 1280 FDA-approved molecules. For each set of drugs from the library one plate was treated with 50 µM cisplatin while the second plate with identical array of drugs was left without cisplatin. Drugs killing the cells only in combination with cisplatin were considered as the hits (red boxes), while drugs inducing cell death per se (black boxes) were excluded. Experiments were performed in triplicates. **(B)** The panel shows outcome of the screening. Average viability of IGROV-CP20 cells in cisplatin was considered as 0 (blue dash line) after normalization. Standard deviation (SD) values of IGROV-CP20 cells in cisplatin were used to normalize the average MTT signal for each drug. All drugs, whose combination with cisplatin caused decrease in viability beyond a threshold of 5 SDs (red dash line), were considered as hits (red circles). **(C)** The graph shows the percentage of viability of IGROVCP20 cells given by the positive hits in combination with cisplatin. **(D)** Quantification of MTT absorbance (as readout of viability) shows dose-response curves of Tranilast, Telmisartan and Amphotericin B added to IGROV-CP20 cells with (red line) or without (blue line) 50 µM cisplatin. Blue dash line shows viability in untreated cells, while red dash line shows viability in the cells treated with cisplatin alone. Data represent average of 6 different experiments**.**

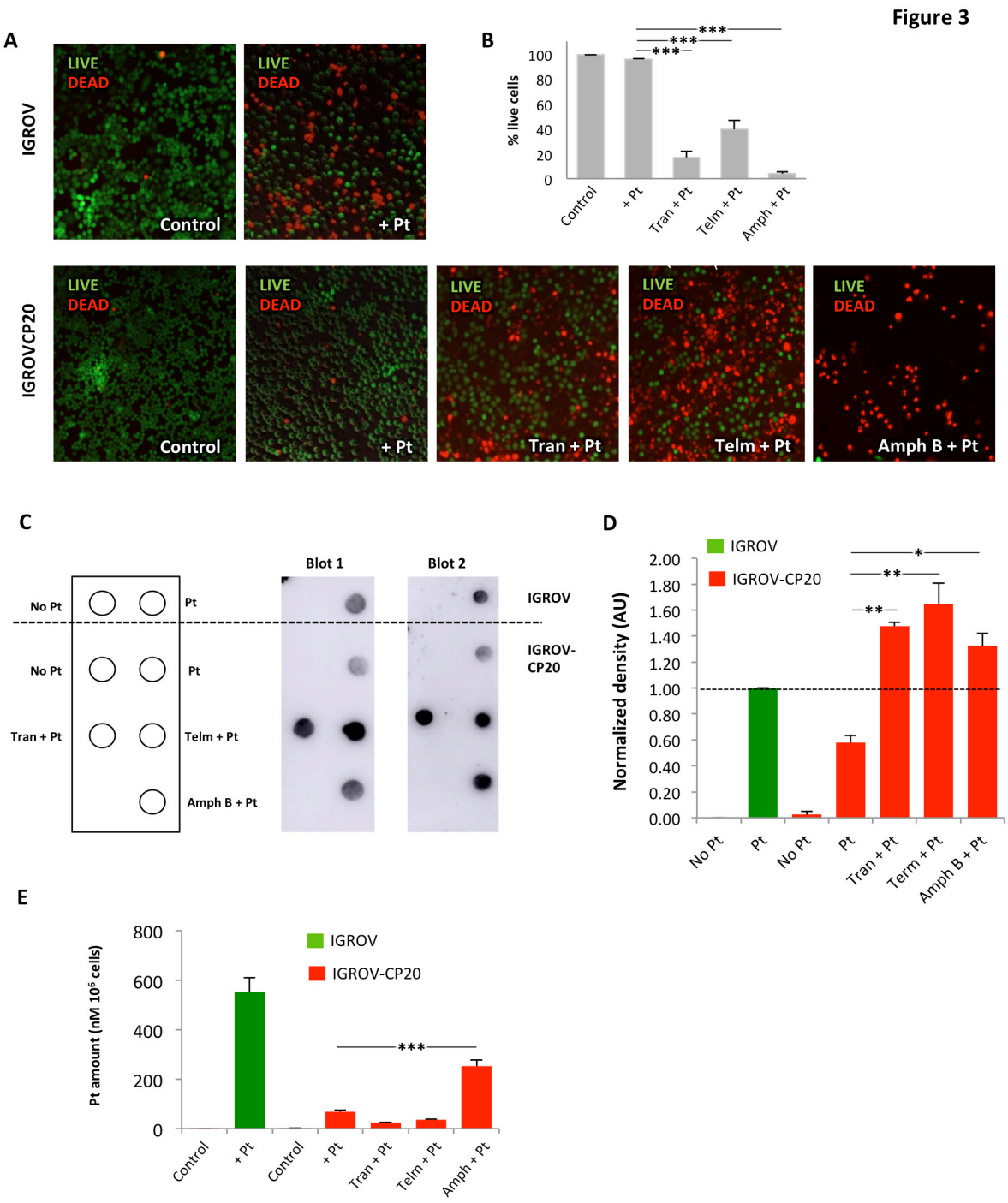

Figure 3: FDA-approved hit drugs promote cisplatin toxicity and stimulate DNA adduct formation in resistant IGROV-CP20 tumor cells.

(A) Representative image of live/dead assay showing the effect of 50µM cisplatin (Pt) on cell viability (dead cells are in red while live cells are in green) of the IGROV or IGROV-CP20 cells as indicated. Pretreatment with 10µM Tranilast, Telmisartan or Amphotericin B for 24h increase cell death of IGROV-CP20 cell when combined with cisplatin. **(B)**. Quantification of experiments shows in panel A reveals significant decrease in viability of IGEROV-CP20 cells treated with mixture of cisplatin and indicated drugs (n=10 fields; ***p<0.001, t-test). **(C)** Pt adducts were evaluated via dot immuno-blot (see methods) in the DNA samples from IGROV cell (above the dash line) and IGROV-CP20 cell (below the dash line), which were spotted as indicated in the membrane map (on the left). Two dot blot images demonstrate that cisplatin (Pt) in association with Tranilast, Telmisartan or Amphotericin B induce a significant increase DNA adducts signal compared to the IGROV-CP20 treated with cisplatin alone **(D)** The graph shows quantification of DNA adduct signal in dot blot experiments (n=10 fields; **p<0.01, *p<0.05, t-test). **(E)** Cell were treated as in panel A and prepared for ICP-MS (see Methods) to evaluate platinum levels in IGROV and IGROV-CP20 cells. Only Amphotericin B combination with cisplatin led to increase in overall platinum levels in the cells . Sensitive cells IGROV (green bars) were used as positive control upon cisplatin treatment. Pt content of each specimen was normalized to the total cell numbers as nM of Pt in 10^6 cells (n=3 experiments; ***p<0.001, t-test)

Figure 4

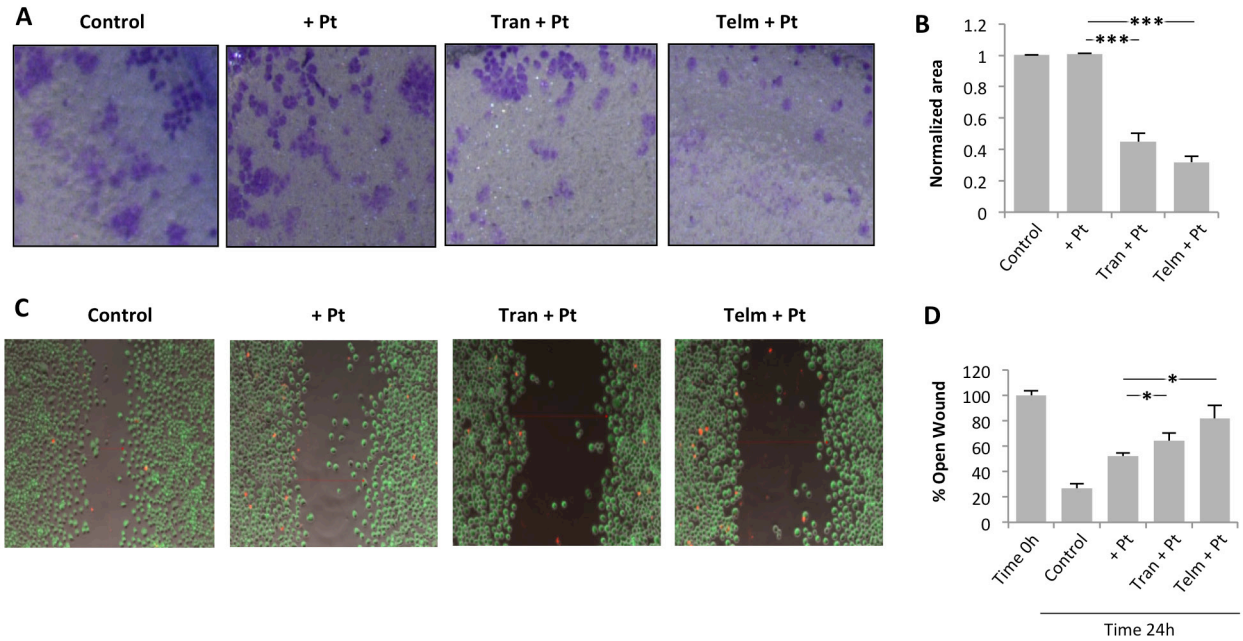

Figure 4. FDA-approved hit drugs slow migration of cisplatin-treated IGROV-CP20 tumor cells.
(A, B) Transwell migration assay (see Methods) was carried out for IGROV-CP20 cells upon treatments with Tranilast or Telmisartan (10 µM) in combination with cisplatin (50 µM) for 24h. Representative pictures of the area of migration (A) were quantified through densitometry (B) to reveal reduced migration in the cells treated the hit drugs combined with cisplatin (n=10 fields; ***$p<0.001$, t-test). **(C, D)** Wound healing assay (see Methods) was performed during in IGROV-CP20 cells for 24h. Cisplatin (50 µM) was added alone or in combination with Tranilast or Telmisartan (10 µM) during wound repair. Both representative images (C) and quantification of remaining open wound (D) revealed ability of both Tranilast and Telmisartan to promote inhibitory impact of cisplatin on wound repopulation (n=3 experiments; *$p<0.05$, t-test).

Figure 5

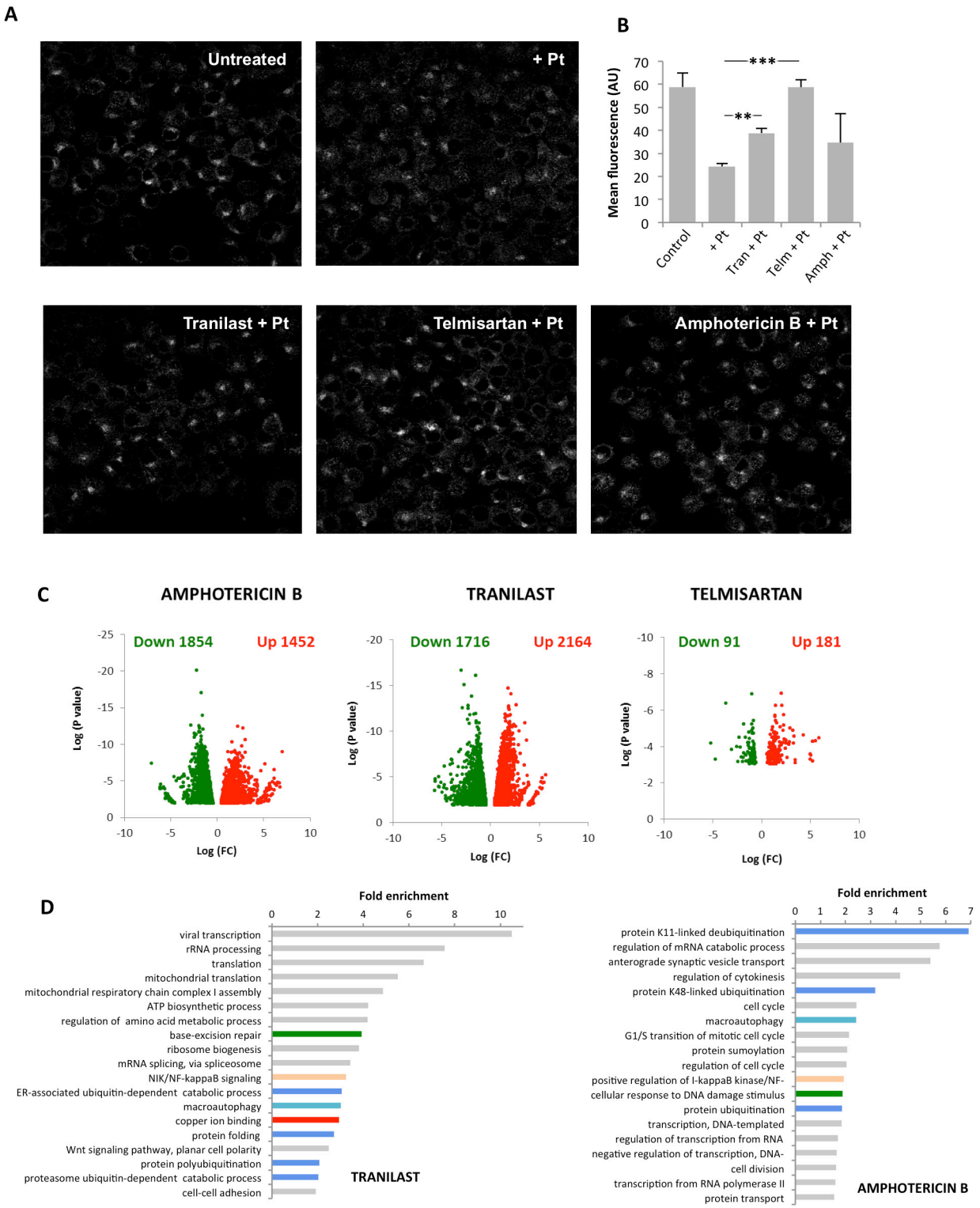

Figure 5. **Impact of drugs on Pt-mediate ATP7B trafficking and on transcriptional response to cisplatin in IGROV-CP20 cells.** **(A, B)** IGROV-CP20 cells were treated with 10µM Tranilast, Telmisartan and Amphotericin B for 24h and then exposed to 50µM cisplatin for 4h to activate ATP7B trafficking. Confocal images (A) show that the drugs promote ATP7B retention in the Golgi upon cisplatin treatment as also revealed by quantification of ATP7B signal (B) in the Golgi region (n=10 fields; **- p<0.01, *** - p<0.001, t-test). **(C)** IGROV-CP20 cells were exposed for 24h to 50µM cisplatin directly or after 24h pretreatment with 10µM Tranilast, Telmisartan and Amphotericin B and prepared for QuantSeq analysis of mRNA (see Methods). Volcano plot diagrams show down and up-regulated genes in IGROV-CP20 cells treated with drugs and cisplatin compared to cisplatin alone. Data are expressed as Log of mRNA fold change. **(D)** The diagrams show outcome of GO enrichment analysis of gene, whose expression was down-regulated by Tranilast or Amphotorecin B in cisplatin-treated cells. Pathways in common between the two drugs are depicted with similar colors with the exception of copper ion binding category (red bar), which have been found only upon Tranilast treatment. DNA repair (green bars); protein quality control, ubiquitination and folding (blue bars); macroautophagy (cyan bars) and NFKB signaling (pink bars) are downregulated pathways in common between the two treatments.

Figure 6

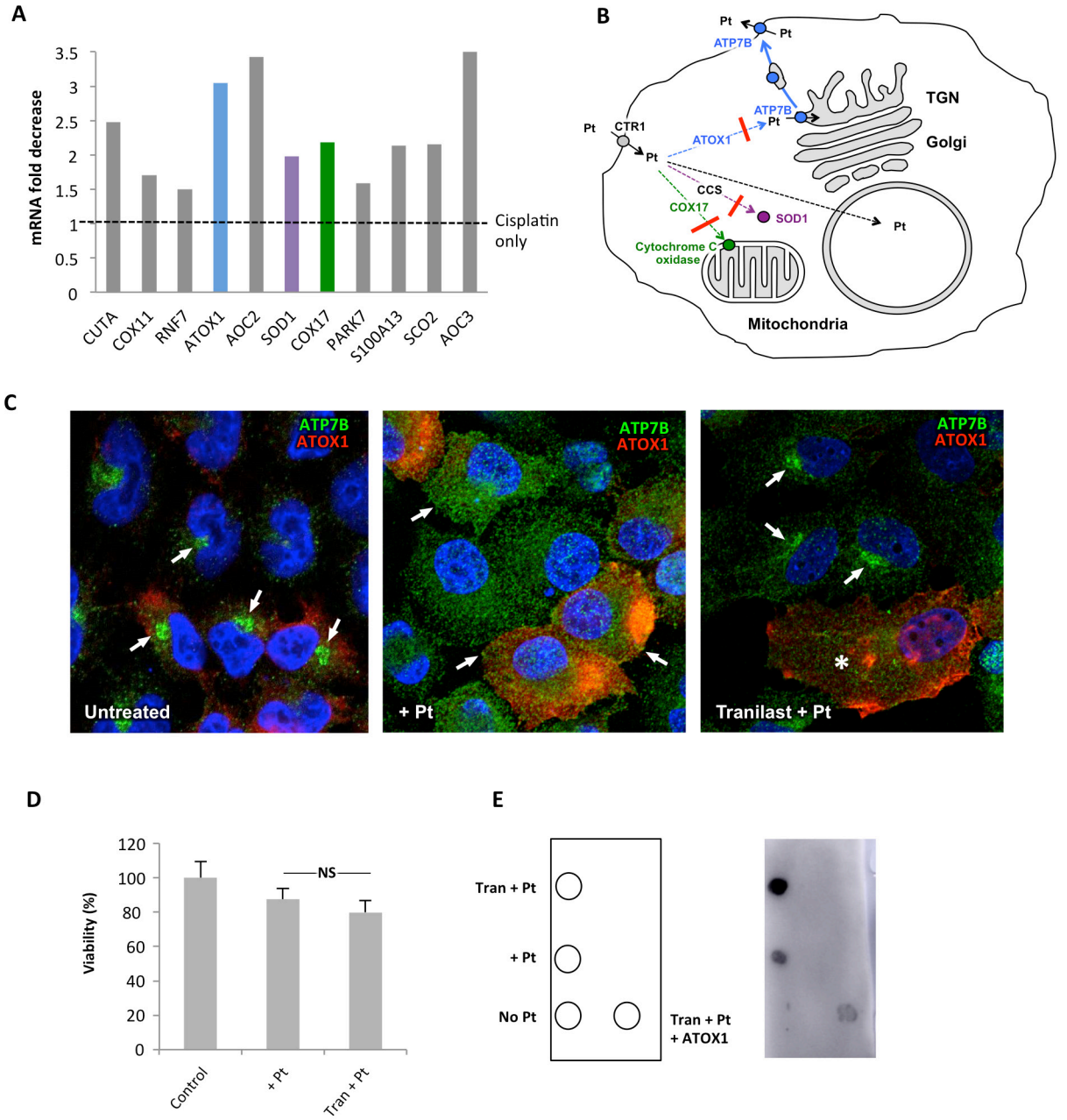

Figure 6. Tranilast suppresses the expression of copper associated genes in ciaplatin-resistant IGROV-CP20 cells

(A) QuantSeq analysis shows Tranilast-mediated fold decrease in the expression the copper ion binding genes in cisplatin-treated IGROV-CP20 cells. The genes, playing a key role in the distribution of Pt across the cell (ATOX1, SOD1 and COX17) are shown in different color corresponding to the specific intracellular destination shown in panel B. **(B)** The scheme show Pt intracellular routes. Down-regulation of ATOX1, SOD1 and COX17 by Tranilast (Red cross-bars) inhibits Pt delivery to secretory pathway (blue arrows), mitochondria (green arrows) or SOD1-mediated detoxification (magenta arrow). This favors delivery of Pt and its accumulation within the cell nucleus (dash black arrow) leading to an enhanced DNA damage followed by apoptosis. **(C)** IGROV-CP20 cells were transfected with a pCDNA-ATOX1-FLAG expression vector and immuno-stained for FLAG (red) antibody and the ATP7B (green) antibody while nuclei stained with DAPI (blue). Cells were treated with 50µM ciaplatin (Pt) or with a combination of 10µM Tranilast and Pt (as indicated in the figure). ATP7B was detected in the Golgi area in untreated cells (arrows, left panel) and at the cell surface and peripheral structures in Pt-treated cells (arrows, mid panel) regardless ATOX1 overexpression. Tranilast blocked ATP7B in the Golgi area in Pt-treated cells, which did not overexpress ATOX1 (arrows, right panel), but failed to affect Pt-mediated redistribution of ATP7B in ATOX1-overexpressing cells (asterisks, right panel). **(D)** MTT viability assay was performed in IGROV-CP20 cells overexpressing ATOX1 and treated with 50 µM cisplatin alone or in combination with 10µM Tranilast. The plot shows that Tranilast did not reduce viability of Pt-treated IGROV-CP20 cells when ATOX1 is overexpressed. **(E)** Pt adducts were evaluated via dot immuno-blot in the DNA samples from IGROV-CP20 cell which were spotted as indicated in the map of the membrane (on the left). Dot blot image demonstrates that cisplatin (Pt) in association with Tranilast induced a significant increase in DNA adducts signal compared to the IGROV-CP20 treated with cisplatin alone. ATOX1 overexpression inhibited ability of Tranilast to promote DNA adduct formation in Pt-treated IGROV-CP20 cells.